

Comparison of OCT and OCTA manifestations among untreated PCV, neovascular AMD, and CSC in Chinese population

Ming-Zhen Yuan, Lu-Lu Chen, Jing-Yuan Yang, Ming-Yue Luo, You-Xin Chen

Department of Ophthalmology, Peking Union Medical College Hospital, Chinese Academy of Medical Sciences and Peking Union Medical College, Beijing 100730, China

Correspondence to: You-Xin Chen. Department of Ophthalmology, Peking Union Medical College Hospital, Chinese Academy of Medical Sciences and Peking Union Medical College, Beijing 100730, China. chenyx@pumch.cn

Received: 2019-08-13 Accepted: 2019-09-17

Abstract

• **AIM:** To compare the qualitative and quantitative features among untreated polypoidal choroidal vasculopathy (PCV), neovascular age-related macular degeneration (nv-AMD) and central serous chorioretinopathy (CSC) using optical coherence tomography (OCT) and OCT angiography (OCTA).

• **METHODS:** This retrospective study included 16 eyes with thin-choroid PCV, 18 eyes with thick-choroid PCV, 16 eyes with nv-AMD and 17 eyes with CSC, respectively. The indicators were obtained by OCT and OCTA.

• **RESULTS:** Sub-foveal choroidal thickness (SFCT) in CSC was thicker compared to other groups (all $P < 0.05$). SFCT in nv-AMD was thicker compared to thin-choroid PCV, but thinner compared with thick-choroid PCV (both $P < 0.05$). As the ratio of thickness of Haller's layer to thickness of SFCT, which of thin-choroid PCV was significantly higher than CSC ($P < 0.001$). Likewise, thick-choroid PCV had significantly higher ratio than nv-AMD ($P = 0.016$) or CSC ($P < 0.001$). There were differences among them in pigment epithelium detachment (PED). The whole-superficial retinal vessel density (RVD), deep RVD and choroidal capillary vessel density (CCVD) in CSC were significantly higher compared to other three groups, respectively (all $P < 0.05$). The whole CCVD in nv-AMD was higher compared to thick-choroid PCV ($P = 0.032$). Cross-sectional local angiographic form was 87.50%, 83.33%, 0 and 35.29% in thin-choroid PCV, thick-choroid PCV, nv-AMD and CSC, respectively. Cross-sectional diffuse angiographic form was 12.50%, 16.67%, 100% and 5.88% in thin-choroid PCV, thick-choroid PCV, nv-AMD and CSC, respectively.

• **CONCLUSION:** Combination of OCT and OCTA can effectively observe the significant alterations existed in PCV, CSC and nv-AMD, and there are distinctive differences among them. The pathogenesis is not exactly the same between PCV and nv-AMD, or PCV and CSC.

• **KEYWORDS:** polypoidal choroidal vasculopathy; neovascular age-related macular degeneration; central serous chorioretinopathy; Haller's layer; vascular density; pigment epithelium detachment

DOI:10.18240/ijo.2020.01.14

Citation: Yuan MZ, Chen LL, Yang JY, Luo MY, Chen YX. Comparison of OCT and OCTA manifestations among untreated PCV, neovascular AMD, and CSC in Chinese population. *Int J Ophthalmol* 2020;13(1):93-103

INTRODUCTION

Polypoidal choroidal vasculopathy (PCV) is a retinal disease initially described by Yannuzzi *et al*^[1] in 1982. It is a common choroidal vascular disease and the prevalence is higher in Asians than in Caucasians^[2-3]. In the early nineties, some experts started regarding PCV as a subtype of neovascular age-related macular degeneration (nv-AMD) or as a specific idiopathic entity^[4-5]. Until now, whether PCV a variant of nv-AMD or not is still controversial, and the pathogenesis of PCV is still unknown.

Recently, with advances in imaging technology, some researchers have proposed the term "pachychoroid" to describe a spectrum of disease that has the features of choroidal thickening, such as PCV, central serous chorioretinopathy (CSC), pachychoroid pigment epitheliopathy, pachychoroid neovascularopathy, and peripapillary pachychoroid syndrome. However, different from other pachychoroid diseases, PCV have a wide range of choroidal thickness and the choroidal thickness does not always thicken in PCV^[6]. In addition, PCV occurring in eyes that lacks typical characteristics of nv-AMD, may be a member of the pachychoroid disease spectrum, which indicates that pachychoroid features may be related to the pathogenesis of PCV in pachychoroid eyes^[6-7]. Plus, many literatures pointed out that the history of CSC is much more

commonly seen in eyes with PCV compared with those with nv-AMD^[8]. Therefore, more and more researchers focus on studying the relationship among PCV, nv-AMD and CSC, especially imaging studies^[6,9-10]. Some researchers believed that choroidal vascular changes accompany the processes of PCV, nv-AMD and CSC. Last year, a previous study by Baek *et al*^[9] demonstrated that there were similarities in vascular density of the large choroidal vessel layer and pachyvessel pattern between CSC and thick-choroid PCV and between nv-AMD and thin-choroid PCV, which implies these three diseases may share common pathophysiology involving choroidal changes. Optical coherence tomography angiography (OCTA) is a recently advanced noninvasive imaging technique that could generate retinal and choroidal quantify vessel density and blood flow^[11]. Many studies illustrated that OCTA would be capable of localizing the site at which a feeder vessel, derived from the choroid or breaking through Bruch's membrane (BM), as well as would provide quantitative assessment with metrics of vessel density, vessel connectivity, which may provide new insight into the pathogenesis of choroidal neovascularization (CNV)^[11-13]. Recently, Kang *et al*^[14] demonstrated the potential possibilities and advantages of using OCTA to assess pigment epithelium detachment (PED) features and detect the presence of neovascular (NV) in PED. However, no data are available to reveal the relationship among these three diseases in OCTA manifestations. Therefore, the purpose of this study analyze them the features qualitatively and quantitatively using OCTA in eyes with untreated PCV, nv-AMD and CSC.

SUBJECTS AND METHODS

Ethical Approval This cross-sectional study was performed at the Department of Ophthalmology in Peking Union Medical College Hospital, Chinese Academy of Medical Sciences in China. The study was approved by the Institutional Review Board of Peking Union Medical College Hospital, which allowed recruitment of patients, review of clinical charts, and the acquisition of OCTA scans performed in a 6×6 mm² area centered on the macula with the Optovue RTVue-XR Avanti with AngioVue. The study was conducted in accordance with the tenets of the Declaration of Helsinki. All participants signed the informed consents and didn't receive any stipends.

Enrollment of Study Subjects We recruited untreated patients with PCV, nv-AMD and CSC who visited our hospital between August 2018 and February 2019. All patients had a standardized history, clinical examination and underwent fluorescein angiography (FA) and indocyanine green angiogram (ICGA) performed with the Heidelberg Spectralis HRA (Heidelberg Engineering, Heidelberg, Germany). Eyes included in the study had a clinical diagnosis of PCV, nv-AMD and CSC based on the clinical history, fundoscopic examination, OCT, FA and ICGA. Study eyes had not received

any previous therapy [laser, photodynamic therapy, or anti-vascular endothelial growth factor (VEGF)] treatment. We divided PCV into two groups according to the sub-foveal choroidal thickness (SFCT) for analyzing the choroidal characteristics of subtypes. Median SFCT (244.5 μm) was used as the cut-off value. Exclusion criteria were as follows: 1) eyes with CNV caused by other than these diseases; 2) any history of previous treatments such as laser photocoagulation, photodynamic therapy, intraocular anti-VEGF therapy, and corticosteroids treatment; 3) other ocular diseases including high myopia (<-6 diopter or axial length >26 mm), diabetic retinopathy, glaucoma, retinal detachment, or uveitis; 4) poor image quality of OCTA and inability to obtain serial imaging.

Image Acquisition and Analysis The quantitative features, like thickness and height, were measured using the horizontal and vertical line scans intersecting the center of the fovea on enhanced depth imaging mode of Spectralis spectral-domain OCT (EDI-OCT). Based on these scans, SFCT was defined as the distance from the BM to the choroid-scleral interface at the fovea after binarization analysis in MATLAB^[15] (Figure 1). The SFCT was defined as the distance between the hyperreflective line of BM and the innermost hyperreflective line of the choroid-scleral interface^[16]. We defined the thickness of Haller's layer as the distance from the innermost point of the largest choroidal vessel closest to the fovea to the inner border of the sclera after binarization analysis in MATLAB^[16] (Figure 1). And then we calculated the ratio of thickness of Haller's layer to thickness of SFCT. Three independent retinal specialists (Yuan MZ, Chen LL and Yang JY) measured these parameters. Furthermore, the whole-superficial retinal vessel density (RVD), the whole-deep RVD and the whole choroidal capillary vessel density (CCVD) were automatically generated by OCTA. Fovea avascular zone (FAZ) was round and intact with a well-demarcated border in retina, which was also measured using OCTA. FAZ perimeter (PERIM) was calculated in base of FAZ. Then we obtained an automated contour evaluation using the built-in "non-flow" area calculator. Each patient underwent two examinations, and finally we took the average value as the measurement result.

The qualitative features, like PED subtype classifications and cross-sectional OCTA classifications, were measured using the horizontal cross-sectional scan. Based on the guidelines provided by Lee *et al*^[17], PEDs were classified independently by three subtypes, including drusenoid PEDs, serous PEDs and vascularized PEDs. As for vascularized PEDs, we defined a "peaked" PED to describe the vascularized having a sharp peak on OCT, and a "flat" PED to describe a shallow and irregular on OCT. In addition to that, drusenoid PEDs were identified as areas of RPE elevation, typically smooth in contour and with medium to high, but homogenous, internal reflectivity. Serous

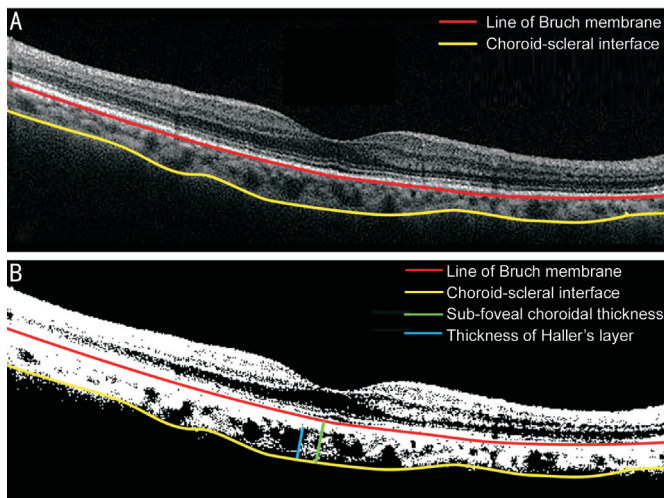


Figure 1 Image binarization for subfoveal choroid A: The image acquired by EDI-OCT; B: Visualization of choroid morphologic and parameters obtained by our custom-written application on MATLAB on image acquired by EDI-OCT.

PEDs were identified as localized, relatively dome-shaped elevations of the RPE band with low internal reflectivity within the PED (optically empty) and good visualization of the underlying BM band and choroid. Representative images of each PED subtype were shown in Figure 2. Besides, we classified the horizontal cross-sectional scans of OCTA into two forms, including cross-sectional local angiographic form and cross-sectional diffuse angiographic form^[18]. As for cross-sectional local angiographic form, one of which was nodular form and another of which was cluster form. Representative images of the horizontal cross-sectional scans on OCTA were shown in Figure 3.

Statistical Analysis Statistical analysis was performed with SPSS statistical software (version 22.0; SPSS Inc., Chicago, IL, USA). The Student's *t*-test and one-way analysis of variance (ANOVA) for continuous variables among and between groups after normal distribution confirmation using the Kolmogorov-Smirnov test. Mann-Whitney tests were used when a normal distribution could not be confirmed. Chi-square test was used to compare the categorical parameters. The coefficient of correlation was determined by Pearson's correlation analysis. A *P* value <0.05 was considered statistically significant.

RESULTS

In this study, we imaged a total of 67 eyes of 65 patients for analysis, 34 eyes with PCV, 16 eyes with nv-AMD, and 17 eyes with CSC. All of these patients were Chinese and treatment naïve. The mean age of patients with PCV was 64.27±7.83y (range, 49-82y), and 22 (64.71%) patients were male. The patients with nv-AMD (68.68±9.38y) were significantly older than those with PCV (*P*=0.032). The mean age of patients with CSC (42.26±9.39y) was younger compared with other two groups (both *P*<0.05; Table 1, Figure 4). There

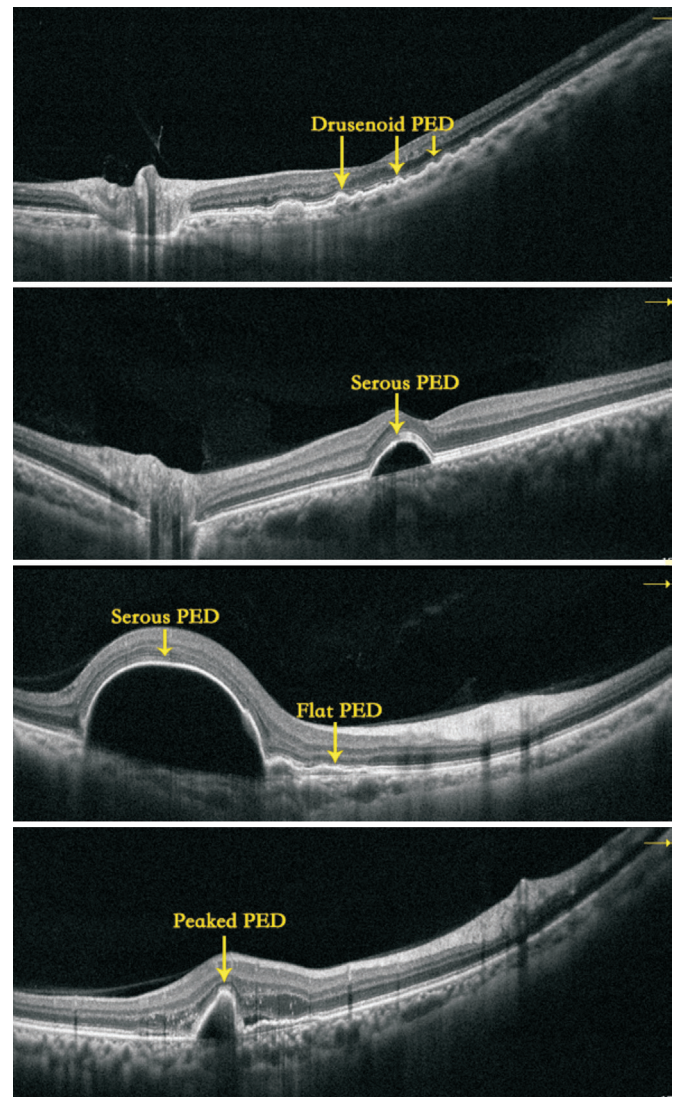


Figure 2 PED subtype classifications, including drusenoid PED, serous PED, flat PED and peaked PED.

was no significant difference in gender. As for PCV, SFCT was >244.5 μm in 18 eyes (thick-choroid PCV) and ≤244.5 μm in 16 eyes (thin-choroid PCV). The mean SFCT was 196.45±43.85 μm, 309.16±47.50 μm, 246.41±83.08 μm, and 376.78±103.57 μm, in thin-choroid PCV, thick-choroid PCV, nv-AMD, and CSC. SFCT in CSC was thicker compared to other groups (all *P*<0.05). SFCT in nv-AMD was thicker than thin-choroid PCV, but thinner than thick-choroid PCV (both *P*<0.05; Table 1, Figure 5).

In terms of choroidal morphology, there was no significant difference in the ratio of thickness of Haller's layer to thickness of SFCT between thin-choroid PCV (0.84%±0.06%) and thick-choroid PCV (0.86%±0.06%; *P*=0.473), or between thin-choroid PCV and nv-AMD (0.78%±0.13%; *P*=0.055), or between nv-AMD and CSC (0.72%±0.11%; *P*=0.260). However, the ratio was significantly higher in eyes with thin-choroid PCV compared with CSC (*P*<0.001). Likewise, thick-choroid PCV had significantly higher ratio than nv-AMD (*P*=0.016) or CSC (*P*<0.001; Table 1, Figure 6).

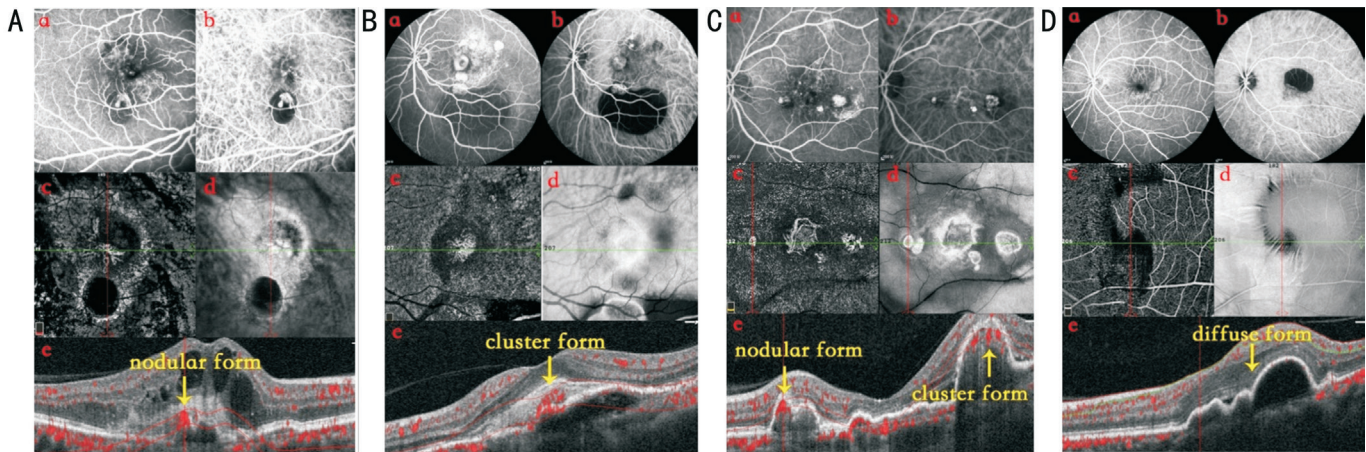


Figure 3 Representative images of the horizontal cross-sectional scans on OCTA A: One PCV patient, there is nodular cross-sectional angiographic form on OCTA; B: One PCV patient, there is cluster cross-sectional angiographic form on OCTA; C: One PCV patient, there are both nodular and cluster cross-sectional angiographic form on OCTA; D: One nv-AMD patient, there is diffuse cross-sectional angiographic form on OCTA. a: Fluorescein angiography; b: Indocyanine green angiogram; c: OCTA; d: Enface form. e: Cross-sectional angiographic form.

Table 1 Baseline characteristics and choroidal morphologic parameters in eyes with thin-choroid PCV, thick-choroid PCV, nv-AMD and CSC

Items	Thin-choroid PCV (SFCT≤244.5 μm, n=16)	Thick-choroid PCV (SFCT>244.5 μm, n=18)	nv-AMD (n=16)	CSC (n=17)
Age, y	66.27±8.13	63.84±7.24	68.68±9.38	42.26±9.39
Gender, male/female (male %)	10/6 (62.5)	12/6 (66.67)	11/5 (68.75)	11/6 (64.71)
SFCT, μm	196.45±43.85	309.16±47.50	246.41±83.08	376.78±103.57
The ratio of Haller's layer thickness to SFCT, %	0.84±0.06	0.86±0.06	0.78±0.13	0.72±0.11
PEDs subtypes, n (%)				
Drusenoid PED	3 (18.8)	3 (16.7)	9 (56.3)	2 (11.8)
Serous PED	9 (56.3)	9 (50)	4 (25)	15 (88.2)
Peaked PED	4 (25)	5 (27.8)	8 (50)	4 (23.5)
Flat PED	14 (87.5)	17 (94.4)	11 (68.6)	2 (11.8)
Quantitative data in OCTA				
Whole superficial RVD, %	46.05±4.43	43.67±3.73	41.84±4.40	50.60±2.87
Whole deep RVD, %	45.86±3.62	44.43±5.26	43.85±4.54	50.70±3.82
Whole CCVD, %	59.61±6.28	56.58±7.57	61.20±5.65	66.00±4.02
FAZ, mm ²	0.34±0.17	0.37±0.14	0.33±0.05	0.26±0.11
PERIM, mm	2.35±0.63	2.25 (2.05, 2.70)	2.28±0.22	2.00 (1.67, 2.29)
The horizontal cross-sectional scans of OCTA, n (%)				
Local angiographic form	14 (87.50)	15 (83.33)	0	6 (35.29)
Diffuse angiographic form	2 (12.50)	3 (16.67)	16 (100)	1 (5.88)

PCV: Polypoidal choroidal vasculopathy; nv-AMD: Neovascular age-related macular degeneration; CSC: Central serous chorioretinopathy; SFCT: Sub-foveal choroidal thickness; PED: Pigment epithelium detachment; OCTA: Optical coherence tomography angiography; RVD: Retinal vessel density; CCVD: Choroidal capillary vessel density; FAZ: Fovea avascular zone; PERIM: FAZ perimeter.

We also researched the PEDs subtypes of different groups in our study. There were 4 patients having only one subtype of PEDs in thin-choroid PCV, 7 patients having only one subtype of PEDs in thick-choroid PCV, 3 patients having only one subtype of PEDs in nv-AMD, 12 patients having only one subtype of PEDs in CSC, respectively. Other patients in these four groups had at least two subtypes of PEDs. Drusenoid PED was associated with nv-AMD (9 eyes, 56.3%), but was

occasionally observed in thin-choroid PCV (3 eyes, 18.8%), thick-choroid PCV (3 eyes, 16.7%) and CSC (2 eyes, 11.8%). Serous PED was closely related to CSC (15 eyes, 88.2%), followed by thin-choroid PCV (9 eyes, 56.3%) and thick-choroid PCV (9 eyes, 50%), but appeared less in nv-AMD (4 eyes, 25%). Peaked PED was a common finding in nv-AMD (8 eyes, 50%), followed by thick-choroid PCV (5 eyes, 27.8%), thin-choroid PCV (4 eyes, 25%), and CSC (4 eyes,

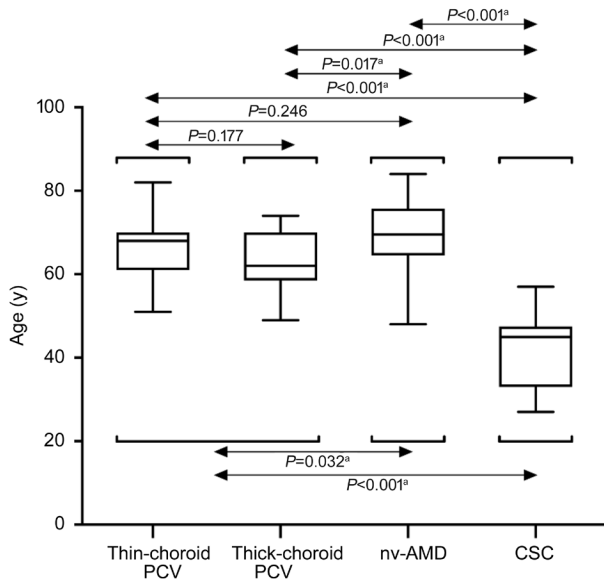


Figure 4 Distribution of age Box plots among thin-choroid PCV, thick-choroid PCV, nv-AMD and CSC. ^a $P<0.05$ was required for results to be considered statistically significant.

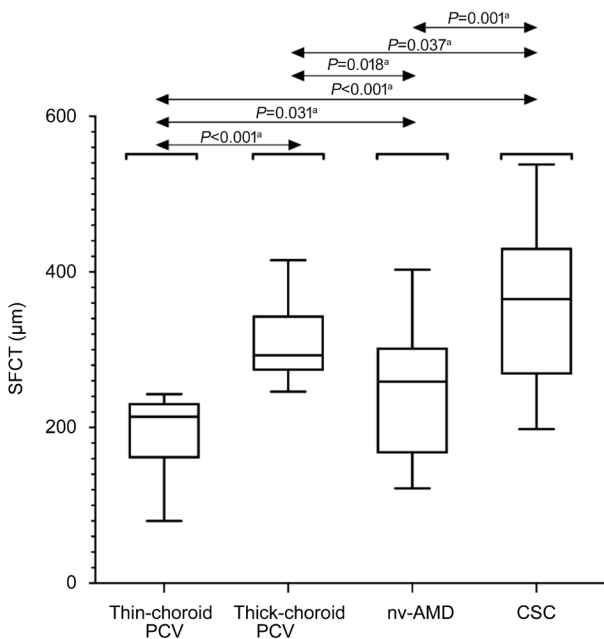


Figure 5 Distribution of SFCT Box plots among thin-choroid PCV, thick-choroid PCV, nv-AMD and CSC. ^a $P<0.05$ was required for results to be considered statistically significant.

23.5%). Flat PED was very common in thin-choroid PCV (14 eyes, 87.5%) and thick-choroid PCV (17 eyes, 94.4%), followed by nv-AMD (11 eyes, 68.6%), but was less likely to appear in CSC (2 eyes, 11.8%; Table 1, Figure 7).

In addition, we also tested some quantitative data in OCTA. The whole-superficial RVD in CSC ($50.60\% \pm 2.87\%$) was higher compared to other three groups (all $P<0.05$). The whole-superficial RVD was significantly higher in eyes with thin-choroid PCV ($46.05\% \pm 4.43\%$) compared with nv-AMD ($41.84\% \pm 4.40\%$; $P=0.029$). However, the difference in the whole-superficial RVD between thick-choroid PCV

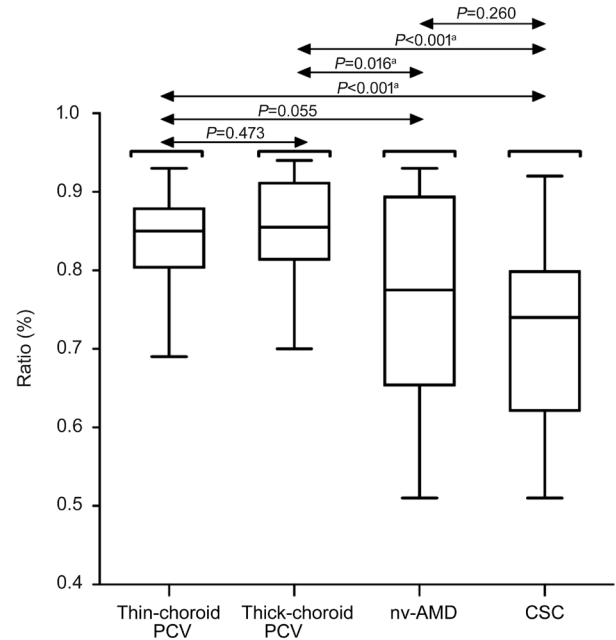


Figure 6 Distribution of the ratio of Haller's layer thickness to SFCT Box plots among thin-choroid PCV, thick-choroid PCV, nv-AMD and CSC. ^a $P<0.05$ was required for results to be considered statistically significant.

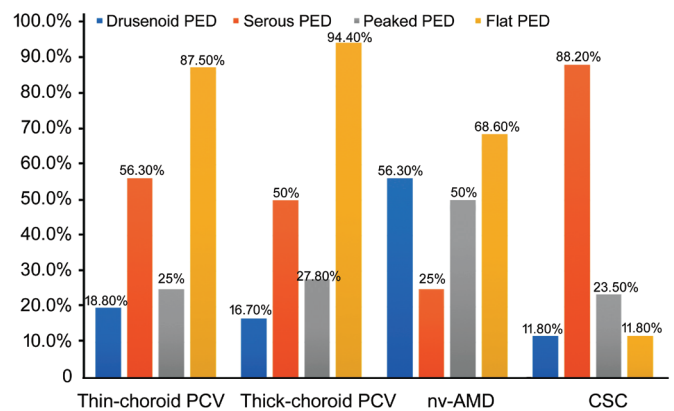


Figure 7 Distribution of each PED subtype among thin-choroid PCV, thick-choroid PCV, nv-AMD and CSC.

($43.67\% \pm 3.73\%$) and thin-choroid PCV ($P=0.192$), or between thick-choroid PCV and nv-AMD ($P=0.225$) was neither statistically significant. Besides, the whole-deep RVD in CSC ($50.70\% \pm 3.82\%$) was higher compared to other three groups (all $P<0.05$). But there was no significant difference in the whole-deep RVD between thin-choroid PCV ($45.86\% \pm 3.62\%$) and thick-choroid PCV ($44.43\% \pm 5.26\%$; $P=0.675$), or between thin-choroid PCV and nv-AMD ($43.85\% \pm 4.54\%$; $P=0.141$), or between thick-choroid PCV and nv-AMD ($P=0.377$). As for the whole CCVD, it was significantly higher in eyes with CSC ($66.00\% \pm 4.02\%$) compared with other three groups (all $P<0.05$). What's more, the whole CCVD in nv-AMD ($61.20\% \pm 5.65\%$) was higher compared to thick-choroid PCV ($56.58\% \pm 7.57\%$; $P=0.032$). But there was no significant difference in the whole CCVD between thin-choroid PCV

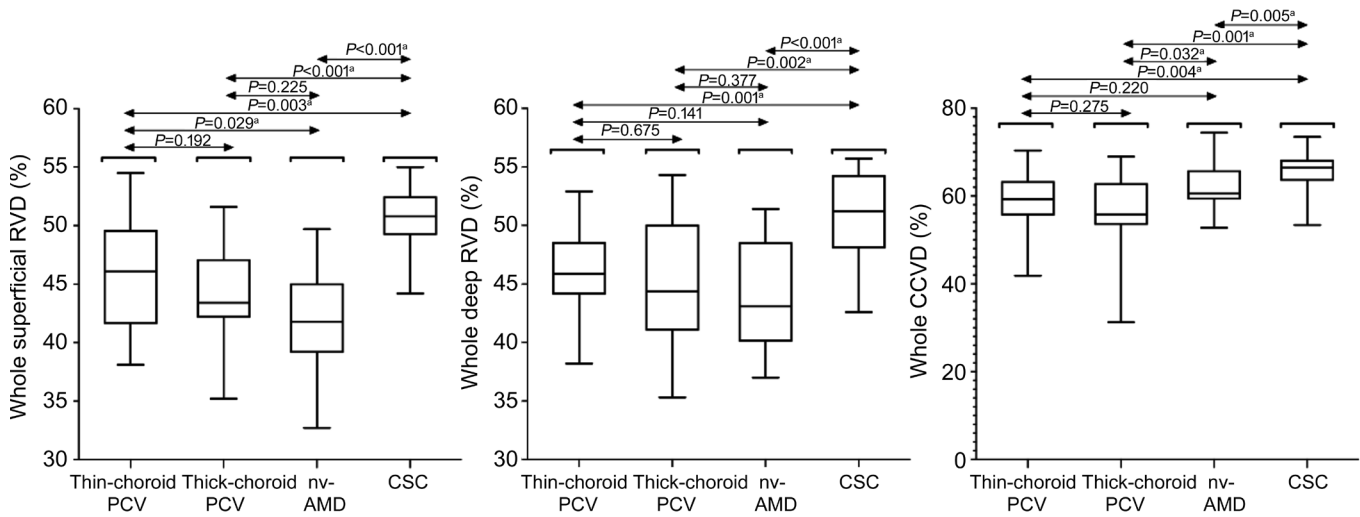


Figure 8 Distribution of the whole superficial RVD, deep RVD and CCVD Box plots among thin-choroid PCV, thick-choroid PCV, nv-AMD and CSC. ^a $P < 0.01$ was required for results to be considered statistically significant.

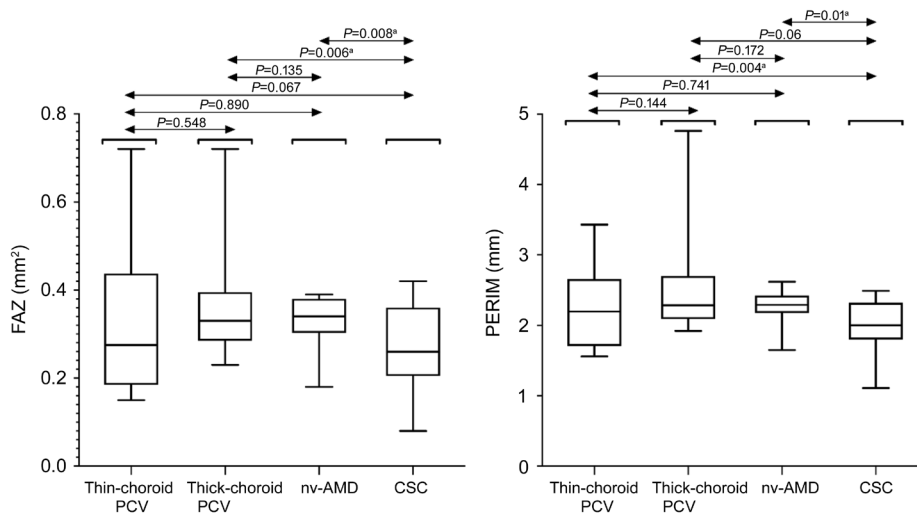


Figure 9 Distributions of FAZ and PERIM Box plots among thin-choroid PCV, thick-choroid PCV, nv-AMD and CSC. ^a $P < 0.01$ was required for results to be considered statistically significant.

(59.61%±6.28%) and thick-choroid PCV ($P=0.275$), or between thin-choroid PCV and nv-AMD ($P=0.220$). Detailed data can be found in the Table 1 and Figure 8. FAZ in CSC ($0.26 \pm 0.11 \text{ mm}^2$) was smaller compared to thick-choroid PCV ($0.37 \pm 0.14 \text{ mm}^2$; $P=0.006$) and nv-AMD ($0.33 \pm 0.05 \text{ mm}^2$; $P=0.008$). There was no significant difference in other groups. In addition, PERIM in CSC 2.00 ($1.67, 2.29$) mm was shorter compared to thin-choroid PCV (2.35 ± 0.63 mm; $P=0.004$) and nv-AMD (2.28 ± 0.22 ; $P=0.01$). There was no significant difference in other groups (Table 1 and Figure 9).

Comparison of the horizontal cross-sectional scans of OCTA showed cross-sectional local angiographic form was 87.50%, 83.33%, 0 and 35.29% in thin-choroid PCV, thick-choroid PCV, nv-AMD and CSC, respectively. Of which, there were 5 PCV patients and 1 CSC patient having cluster cross-sectional local angiographic form, 1 PCV patient having both nodular

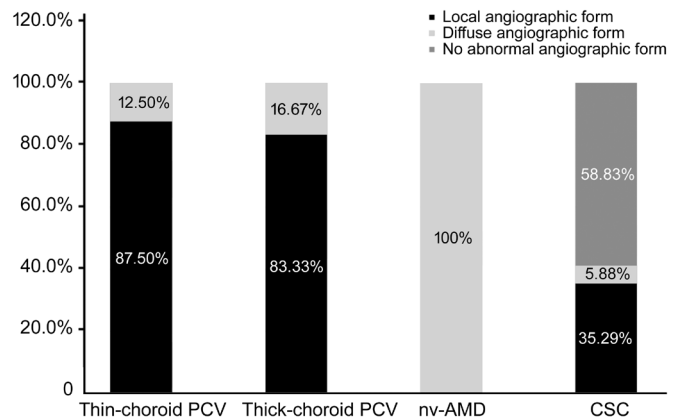


Figure 10 Distribution of different horizontal cross-sectional scans of OCTA among thin-choroid PCV, thick-choroid PCV, nv-AMD and CSC.

and cluster cross-sectional local angiographic form, others having nodular cross-sectional local angiographic form. And

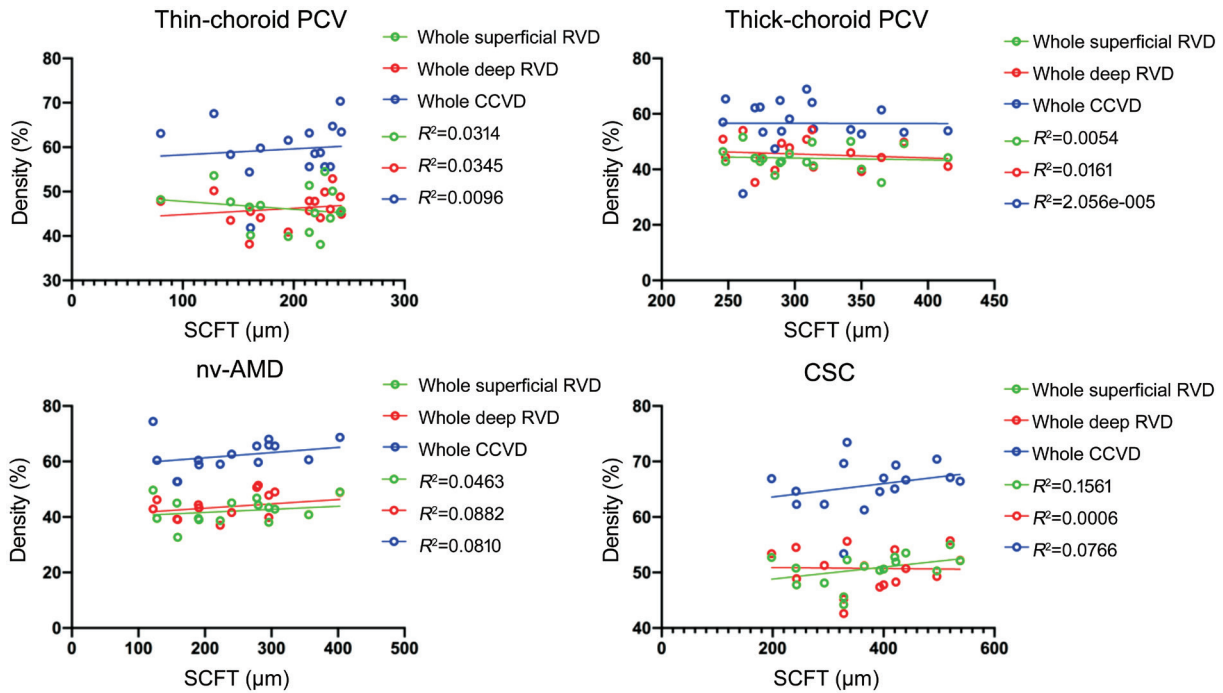


Figure 11 Relationship between vascular density and SFCT Scatter plot showing the correlation was not statistically significant in all these four groups (all $P>0.05$).

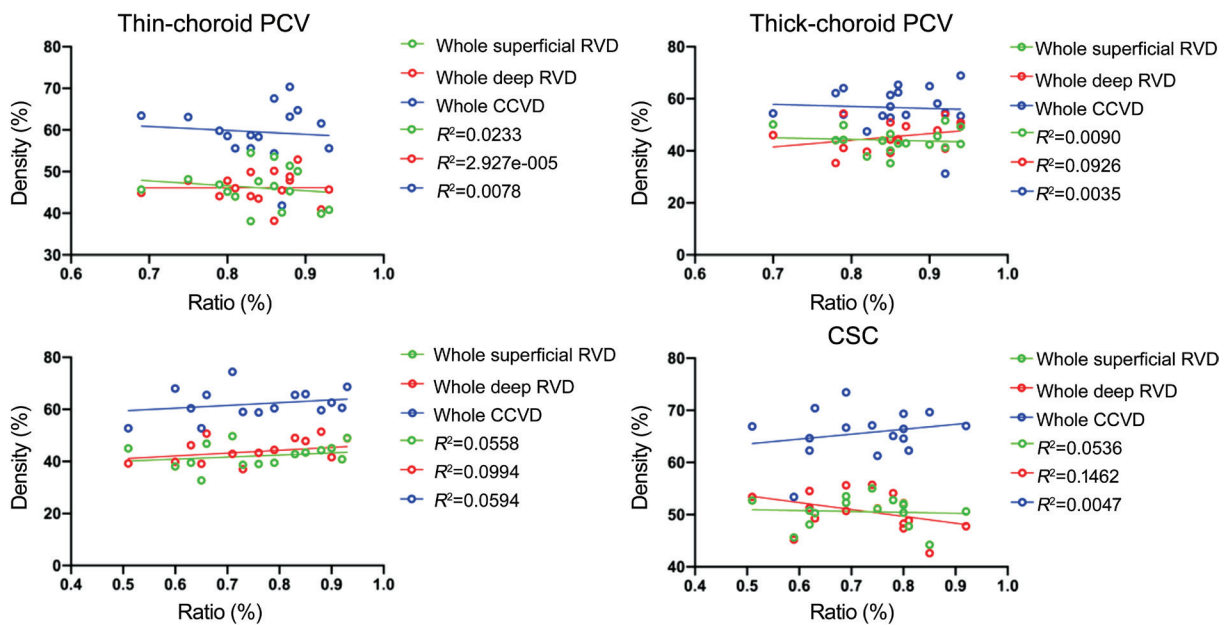


Figure 12 Relationship between vascular density and the ratio of Haller's layer to SFCT Scatter plot showing the correlation was not statistically significant in all these four groups (all $P>0.05$).

morphology was “cross-sectional diffuse angiographic form” was 12.50%, 16.67%, 100% and 5.88% in thin-choroid PCV, thick-choroid PCV, nv-AMD and CSC, respectively (Table 1 and Figure 10).

As for the correlation analysis, we analyzed the correlation between SFCT and whole superficial RVD, whole deep RVD, whole CCVD, respectively. We also analyzed the correlation between the ratio of thickness of Haller's layer to thickness of SFCT and whole superficial RVD, whole deep RVD, whole

CCVD, respectively. The results showed that the correlations were not statistically significant in all these groups (all $P>0.05$). Detailed data can be found in Figures 11, 12.

DISCUSSION

In our study, we compared the qualitative and quantitative characteristics among PCV, nv-AMD and CSC by OCT and OCTA. First, the results showed that SFCT in CSC was thicker compared to other three groups. This result is consistent with previous studies which suggest that pachychoroid

pigment epitheliopathy is thought to be a form of CSC^[19-20]. Interestingly, we found that some PCV patients had thicker choroid than nv-AMD, but there were still PCV patients with thinner choroid than nv-AMD. As for SFCT, some researchers believed that increased choroidal hyperpermeability caused by choroidal thickening was important for the pathogenesis of PCV, which suggested that the choroidal vascular lesion seen in PCV may have a significant structural difference in the choroid compared to nv-AMD^[21-22]. However, our study found that not all SFCT in patients with PCV were thicker than nv-AMD. There are two points in our analysis. First, there are many factors affecting choroidal thickness, such as age, gender, axial length, and systemic diseases^[23-25], which will affect the measurement and comparison of choroidal thickness. Secondly, as choroidal thickening could increase choroidal hyperpermeability, we consider SFCT of patients with PCV may be related to the severity or duration of disease, which may explain that not all patients with PCV have the characteristic of choroidal thickening. Therefore, the research on the role of SFCT in PCV and nv-AMD remains to be further studied. In addition to SFCT, Haller vessel dilatation with choriocapillaris attenuation in these diseases has aroused extensive concentration. Recently, one study found that diffuse homogeneous Haller's vessel dilatation accompanied with choriocapillaris attenuation was identified around the disease foci in CSC, which was similar to those seen in PCV with thick choroid^[9]. What's more, another study said that dilation of large choroidal vessels were more commonly seen in PCV patients than nv-AMD^[26]. In our study, we analyzed the ratio of thickness of Haller's layer to thickness of SFCT among these four groups. The result showed the ratio of Haller's layer to thickness of SFCT from high to low was thick PCV, thin PCV, CSC and nv-AMD, which was not exactly the same as the previous studies. For this result, we speculated that dilated Haller's layer vessels appeared more often in PCV patients and CSC patients, supporting the theory that PCV may be one of the pachychoroid spectrum disorders and should be distinguished from nv-AMD.

With the development of OCT technology, we could use this technology to segment and quantify RPE elevations. Currently, PED subtypes are generally classified into drusenoid PEDs, Serous PEDs, vascularized PEDs and mix PEDs^[14]. Drusenoid PED is characterized by displacement of RPE away from BM and are homogenous and internal drusen reflectance^[27-28]. In our study, drusenoid PED was mostly associated with nv-AMD, but was occasionally observed in thin-choroid PCV, thick-choroid PCV and CSC. This result indicated that drusenoid PED could be a recognized phenotypic manifestation of AMD, which is similar to previous studies^[29-31]. Serous PED was first

described by Gass^[32] and was known as well-defined, dome-shaped RPE elevations with low internal reflectance and properly good visualization of the underlying BM and choroid. The height and length of serous PED fluctuate from tens of micrometers to several millimeters, and there are different types of forms, including round, oval, horseshoe-shaped^[19,33-34]. In our research, serous PED was closely related to CSC, followed by thin-choroid PCV and thick-choroid PCV, but appeared less in nv-AMD. Based on this result, we suggested that serous PED may be a prominent characteristic of CSC and it may play an important role in evaluating the severity and progression of chorioretinal impairment. And secondly, we found that PCV frequently accompanied highly reflective materials within the serous PED beneath the outer surface of the RPE, which indicated the presence of neovascularization (Figure 3). According to previous studies, vascularized PEDs were characteristic of heterogenous internal reflectance in the high or shallow RPE elevations. Peaked PEDs were defined as PEDs with a high peak or a steep angle with a relatively normal contour; those PEDs with a shallow peak and irregular shape were categorized as "flat" PEDs^[35]. Owing to our study, we found that peaked PED was a common finding in nv-AMD followed by thin-choroid PCV, thick-choroid PCV and CSC. Flat PED was very common in thin-choroid PCV and thick-choroid PCV, followed by nv-AMD, but was less likely to appear in CSC. This suggested that although both PCV and nv-AMD had CNV, their development process and manifestations were not exactly the same. However, the specific mechanism remains to be further studied.

As for vascular density, the whole-superficial RVD, deep RVD and CCVD were all significantly higher in eyes with CSC compared with other groups, which was consistent with those of a previous study by Baek *et al*^[9]. Besides, FAZ in CSC was significantly smaller compared to thick choroid and nv-AMD, and PERIM in CSC was significantly shorter compared to thin-choroid PCV and nv-AMD. These results suggested that the CNV of PCV and nv-AMD might share a similar pathophysiology associated with decreased vascular density. However, there was a difference on the whole CCVD indicator between PCV and nv-AMD, like, the whole CCVD in nv-AMD was significantly higher compared to thick-choroid PCV, but not higher than thin-choroid PCV. This result corresponded to the ratio of thickness of Haller's layer to thickness of SFCT among thin-choroid PCV, thick-choroid PCV and nv-AMD. Based on these results, we believed that there was continuous expansion of Haller's layer vessels and gradual choriocapillaris attenuation with the progress of PCV, which didn't exist in nv-AMD. On the above basis, we analyzed the correlation between SFCT and whole superior RVD, whole deep RVD,

whole CCVD, respectively, and also studied the correlation between the ratio of thickness of Haller's layer to thickness of SFCT and whole superior RVD, whole deep RVD, whole CCVD, respectively. The results showed that the correlations were not statistically significant in all these groups, which wasn't exactly the same as a previous study by Baek *et al*^[9]. For this result, there were two possible reasons, one of which may be that our two methods of calculating vascular density were different. Another was that there was sample selection difference between us. Therefore, the research on the correlation between vascular density and SFCT, or the ratio of thickness of Haller's layer to thickness of SFCT remains to be further studied.

In addition to this, we compared the horizontal cross-sectional scans of OCTA among them, which showed OCTA can detect vascular network in the majority of cases with PCV and nv-AMD, but there were differences between them. Cross-sectional local angiographic form was commonly in PCV, including cluster cross-sectional local angiographic form and nodular cross-sectional local angiographic form; however, cross-sectional diffuse angiographic form was commonly in nv-AMD. Combine the analysis of ICGA, we believed the above local cross-sectional local angiographic form represented the polypoidal lesions in PCV, which was consistent with other research results^[36-39]. Therefore, OCTA combined with cross-sectional OCT could provide more comprehensive picture of PCV, which may help ophthalmologists to generate prompt diagnosis of PCV, and provided ophthalmologists a good way to distinguish between PCV and nv-AMD.

There are several limitations our study. The sample size was relatively small. And owing to the differences in age between study groups, we did not include a normal population as controls. Besides, our subjects were all from the Chinese population, as well as we did not measure axial length of study eyes. In addition to this, the research indicators we selected are more cumbersome, therefore, in the future research, we will conduct in-depth research and analysis on the more meaningful indicators in the results of this article.

All in all, combination of OCT and OCTA can effectively observe the significant alterations in retinal and choroidal manifestations existed in PCV, CSC and nv-AMD, and there are distinctive differences among them. Besides, there is gradual thickening of the choroid, continuous expansion of Haller's layer vessels and gradual choriocapillaris attenuation with the progress of PCV, which didn't exist in CSC or nv-AMD. Also, compared with CSC and nv-AMD, PCV has the unique characteristic of cross-sectional local angiographic form on OCTA. Therefore, we can't simply think that the pathophysiology of PCV and nv-AMD is similar, or PCV and

CSC shared a similar pathophysiology. We believe this study will improve deeper understanding of the pathogenesis of PCV and provide a more reasonable diagnosis and treatment plan for PCV.

ACKNOWLEDGEMENTS

Thanks to Peking Union Medical College Hospital for providing me with a good learning environment. I am grateful to Prof. Chen YX for giving me the opportunity to study for a doctor. Thank you for the cooperation and support from every patient. Finally, thanks to the encouragement and companionship of parents and husband.

Foundation: Supported by National Natural Science Foundation of China (No.81670879).

Conflicts of Interest: Yuan MZ, None; Chen LL, None; Yang JY, None; Luo MY, None; Chen YX, None.

REFERENCES

- 1 Yannuzzi LA, Sorenson JOHN, Spaide RF, Lipson BARRY. Idiopathic polypoidal choroidal vasculopathy (PCV). *Retina* 1990;10(1):1-8.
- 2 Wong WL, Su XY, Li X, Cheung CM, Klein R, Cheng CY, Wong TY. Global prevalence of age-related macular degeneration and disease burden projection for 2020 and 2040: a systematic review and meta-analysis. *Lancet Glob Health* 2014;2(2):e106-e116.
- 3 Laude A, Cackett PD, Vithana EN, Yeo IY, Wong D, Koh AH, Wong TY, Aung T. Polypoidal choroidal vasculopathy and neovascular age-related macular degeneration: same or different disease? *Prog Retin Eye Res* 2010;29(1):19-29.
- 4 Spaide RF, Yannuzzi LA, Slakter JS, Sorenson J, Orlach DA. Indocyanine green videoangiography of idiopathic polypoidal choroidal vasculopathy. *Retina* 1995;15(2):100-110.
- 5 Yannuzzi LA, Ciardella A, Spaide RF, Rabb M, Freund KB, Orlock DA. The expanding clinical spectrum of idiopathic polypoidal choroidal vasculopathy. *Arch Ophthalmol* 1997;115(4):478-485.
- 6 Lee WK, Baek J, Dansingani KK, Lee JH, Freund KB. Choroidal morphology in eyes with polypoidal choroidal vasculopathy and normal or subnormal subfoveal choroidal thickness. *Retina* 2016;36(Suppl 1): S73-S82.
- 7 Baek J, Dansingani KK, Lee JH, Lee WK, Freund KB. Choroidal morphology in eyes with peripapillary polypoidal choroidal vasculopathy. *Retina* 2019;39(8):1571-1579.
- 8 Toyama T, Ohtomo K, Noda Y, Ueta T. Polypoidal choroidal vasculopathy and history of central serous chorioretinopathy. *Eye (Lond)* 2014;28(8):992-997.
- 9 Baek J, Lee JH, Jung BJ, Kook L, Lee WK. Morphologic features of large choroidal vessel layer: age-related macular degeneration, polypoidal choroidal vasculopathy, and central serous chorioretinopathy. *Graefes Arch Clin Exp Ophthalmol* 2018;256(12):2309-2317.
- 10 Chung SE, Kang SW, Lee JH, Kim YT. Choroidal thickness in polypoidal choroidal vasculopathy and exudative age-related macular degeneration. *Ophthalmology* 2011;118(5):840-845.

- 11 Jia YL, Bailey ST, Wilson DJ, Tan O, Klein ML, Flaxel CJ, Potsaid B, Liu JJ, Lu CD, Kraus MF, Fujimoto JG, Huang D. Quantitative optical coherence tomography angiography of choroidal neovascularization in age-related macular degeneration. *Ophthalmology* 2014;121(7):1435-1444.
- 12 Jia YL, Tan O, Tokayer J, Potsaid B, Wang YM, Liu JJ, Kraus MF, Subhash H, Fujimoto JG, Hornegger J, Huang D. Split-spectrum amplitude-decorrelation angiography with optical coherence tomography. *Opt Express* 2012;20(4):4710-4725.
- 13 Kuehlewein L, Bansal M, Lenis TL, Iafe NA, Sadda SR, Bonini Filho MA, De Carlo TE, Waheed NK, Duker JS, Sarraf D. Optical coherence tomography angiography of type 1 neovascularization in age-related macular degeneration. *Am J Ophthalmol* 2015;160(4):739-748.e2.
- 14 Kang H, Byeon SH, Kim SS, Koh HJ, Lee SC, Kim M. Combining en face optical coherence tomography angiography with structural optical coherence tomography and blood flow analysis for detecting choroidal neovascular complexes in pigment epithelial detachments. *Retina* 2019;39(8):1551-1561.
- 15 Branchini LA, Adhi M, Regatieri CV, Nandakumar N, Liu JJ, Laver N, Fujimoto JG, Duker JS. Analysis of choroidal morphologic features and vasculature in healthy eyes using spectral-domain optical coherence tomography. *Ophthalmology* 2013;120(9):1901-1908.
- 16 Staurengi G, Sadda S, Chakravarthy U, Spaide RF; International Nomenclature for Optical Coherence Tomography (IN•OCT) Panel. Proposed lexicon for anatomic landmarks in normal posterior segment spectral-domain optical coherence tomography: the IN•OCT consensus. *Ophthalmology* 2014;121(8):1572-1578.
- 17 Lee SY, Stetson PF, Ruiz-Garcia H, Heussen FM, Sadda SR. Automated characterization of pigment epithelial detachment by optical coherence tomography. *Invest Ophthalmol Vis Sci* 2012;53(1):164-170.
- 18 Gupta P, Ting DSW, Thakku SG, Wong TY, Cheng CY, Wong E, Mathur R, Wong D, Yeo I, Gemmy Cheung CM. Detailed characterization of choroidal morphologic and vascular features in age-related macular degeneration and polypoidal choroidal vasculopathy. *Retina* 2017;37(12):2269-2280.
- 19 Daruich A, Matet A, Dirani A, Bousquet E, Zhao M, Farman N, Jaisser F, Behar-Cohen F. Central serous chorioretinopathy: recent findings and new physiopathology hypothesis. *Prog Retin Eye Res* 2015;48:82-118.
- 20 Dansingani KK, Balaratnasingam C, Naysan J, Freund KB. En face imaging of pachychoroid spectrum disorders with swept-source optical coherence tomography. *Retina* 2016;36(3):499-516.
- 21 Koizumi H, Yamagishi T, Yamazaki T, Kawasaki R, Kinoshita S. Subfoveal choroidal thickness in typical age-related macular degeneration and polypoidal choroidal vasculopathy. *Graefes Arch Clin Exp Ophthalmol* 2011;249(8):1123-1128.
- 22 Ting DS, Ng WY, Ng SR, Tan SP, Yeo IY, Mathur R, Chan CM, Tan AC, Tan GS, Wong TY, Cheung CM. Choroidal thickness changes in age-related macular degeneration and polypoidal choroidal vasculopathy: A 12-month prospective study. *Am J Ophthalmol* 2016;164:128-136.e1.
- 23 Manjunath V, Taha M, Fujimoto JG, Duker JS. Choroidal thickness in normal eyes measured using Cirrus HD optical coherence tomography. *Am J Ophthalmol* 2010;150(3):325-329.e1.
- 24 Margolis R, Spaide RF. A pilot study of enhanced depth imaging optical coherence tomography of the choroid in normal eyes. *Am J Ophthalmol* 2009;147(5):811-815.
- 25 Ding XY, Li JQ, Zeng J, Ma W, Liu R, Li T, Yu SS, Tang SB. Choroidal thickness in healthy Chinese subjects. *Invest Ophthalmol Vis Sci* 2011;52(13):9555-9560.
- 26 Lai KB, Zhou LJ, Zhong XJ, Huang CX, Gong YJ, Xu FB, Ma L, Chen GD, Cheng L, Lu L, Jin CJ. Morphological difference of choroidal vasculature between polypoidal choroidal vasculopathy and neovascular AMD on OCT: from the perspective of pachychoroid. *Ophthalmic Surg Lasers Imaging Retina* 2018;49(10):e114-e121.
- 27 Yu JJ, Agrón E, Clemons TE, Domalpally A, van Asten F, Keenan TD, Cukras C, Chew EY; Age-Related Eye Disease Study Research Group. Natural history of drusenoid pigment epithelial detachment associated with age-related macular degeneration: age-related eye disease study 2 report No. 17. *Ophthalmology* 2019;126(2):261-273.
- 28 Mrejen S, Sarraf D, Mukkamala SK, Freund KB. Multimodal imaging of pigment epithelial detachment: a guide to evaluation. *Retina* 2013;33(9):1735-1762.
- 29 Balaratnasingam C, Yannuzzi LA, Curcio CA, Morgan WH, Querques G, Capuano V, Souied E, Jung J, Freund KB. Associations between retinal pigment epithelium and drusen volume changes during the lifecycle of large drusenoid pigment epithelial detachments. *Invest Ophthalmol Vis Sci* 2016;57(13):5479-5489.
- 30 Zanzottera EC, Messinger JD, Ach T, Smith RT, Curcio CA. Subducted and melanotic cells in advanced age-related macular degeneration are derived from retinal pigment epithelium. *Invest Ophthalmol Vis Sci* 2015;56(5):3269-3278.
- 31 Schlanitz FG, Baumann B, Kundi M, Sacu S, Baratsits M, Scheschy U, Shahlaee A, Mittermüller TJ, Montuoro A, Roberts P, Pircher M, Hitznerberger CK, Schmidt-Erfurth U. Drusen volume development over time and its relevance to the course of age-related macular degeneration. *Br J Ophthalmol* 2017;101(2):198-203.
- 32 Gass JD. Drusen and disciform macular detachment and degeneration. *Trans Am Ophthalmol Soc* 1972;70:409-436.
- 33 V Pasychnikova N, A Naumenko V, R Korol A, S Zadorozhnyy O, B Kustrin T, O Nasinnyk I. Serous pigment epithelium detachment associated with age-related macular degeneration: a possible treatment approach. *Med Hypothesis Discov Innov Ophthalmol* 2012;1(4):72-75.
- 34 Song IS, Shin YU, Lee BR. Time-periodic characteristics in the morphology of idiopathic central serous chorioretinopathy evaluated by volume scan using spectral-domain optical coherence tomography. *Am J Ophthalmol* 2012;154(2):366-375.e4.

- 35 Tan ACS, Simhaee D, Balaratnasingam C, Dansingani KK, Yannuzzi LA. A perspective on the nature and frequency of pigment epithelial detachments. *Am J Ophthalmol* 2016;172:13-27.
- 36 Srour M, Querques G, Semoun O, El Ameen A, Miere A, Sikorav A, Zambrowski O, Souied EH. Optical coherence tomography angiography characteristics of polypoidal choroidal vasculopathy. *Br J Ophthalmol* 2016;100(11):1489-1493.
- 37 Inoue M, Balaratnasingam C, Freund KB. Optical coherence tomography angiography of polypoidal choroidal vasculopathy and polypoidal choroidal neovascularization. *Retina* 2015;35(11):2265-2274.
- 38 Cheung CMG, Yanagi Y, Mohla A, Lee SY, Mathur R, Chan CM, Yeo I, Wong TY. Characterization and differentiation of polypoidal choroidal vasculopathy using swept source optical coherence tomography angiography. *Retina* 2017;37(8):1464-1474.
- 39 Yanagi Y, Mohla A, Lee WK, Lee SY, Mathur R, Chan CM, Yeo I, Wong TY, Cheung CMG. Prevalence and risk factors for nonexudative neovascularization in fellow eyes of patients with unilateral age-related macular degeneration and polypoidal choroidal vasculopathy. *Invest Ophthalmol Vis Sci* 2017;58(9):3488-3495.